This article has been accepted for publication in a future issue of this journal, but has not been fully edited. Content may change prior to final publication. Citation information: DOI 10.1109/LCSYS.2019.2929159, IEEE Control Systems Letters

An Optimized Input/Output-Constrained Control Design with Application to Microgrid Operation

Roland Harvey, *Student Member, IEEE*, Zhihua Qu, *Fellow, IEEE*, and Toru Namerikawa, *Senior Member, IEEE*

***Abstract*—In this paper, a nonlinear control design is presented for systems whose input and output vectors are saturated. The proposed synthesis includes an optimal tracker as the seed controller and explicitly imposes all the relevant constraints on system input, on the rate of change in the input, and on system output by using the tools of barrier functions, input-output feedback linearization, comparison argument, Lyapunov argument, and a real-time constrained optimization. The proposed design is applied to microgrid operation with high penetration of renewable generation, where net load and variable generation must be balanced and the microgrid should be operated at an optimal or near-optimal performance level. Since traditional generation has a limited ramping rate, battery storage devices and demand responses become necessary to effectively deal with variability of renewable generation and to maintain frequency stability, but their capacities are also limited. It is shown that the proposed design is effective for coordinated control of traditional generation, storage and demand response so that the power system frequency is guaranteed to be within the required operational limits and that renewable curtailment is eliminated or minimized.**

***Index Terms*—Constrained control, optimal control, power systems**

I. Introduction

OPTIMAL control theory has been widely applied since the 1950s, and modern control units can perform real-time computation of static optimization, but nonlinear optimal control problems involve dynamic optimization that are generally too difficult to solve computationally online. Hence, nonlinear controls need to be analytically designed and examined. Nonlinear dynamics such as saturation arise naturally in practical applications due to safety and performance requirements as well as physical constraints. Control applications include hybrid vehicle control [1], underwater autonomous vehicles [2], magnetic levitation [3], and power systems [4]. In particular, the problem of designing a real-time optimized control for systems with output, input, and their rate constraints simultaneously has not been addressed.

Barrier functions provide an effective tool to deal with constraints in dynamic systems. Existing results include open-loop techniques [5], barrier approximations [6], and Boolean compositions [7]. Using input-output feedback linearization in conjunction with a comparison argument, a barrier function method is presented in [8] to design feedback control for output constrained systems. While this result has salient features of being analytical and using real-time optimization, it does not consider constraints on the input or its rate of change. It is well known that, as constraints on control input limit control authority, input constraints impede both stability and performance and hence cannot simply be added without adequate design or thorough analysis. Furthermore, none of the existing results have considered tracking or optimal performance.

In this paper, the class of input-output saturated systems with nominal linear dynamics is considered, and a nonlinear optimized control design is presented. Nonlinear stability conditions are derived in closed form for the class of systems by using the Lyapunov direct method and by utilizing the fact that the Jacobian of saturated linear dynamics is piecewise constant, and the conditions can analytically be verified. Additionally, input-to-state stability is also established to ensure robustness of the closed loop system against exogenous input and modeling/prediction errors. The proposed control synthesis methodology embeds the linear quadratic optimal control into a point-wise constrained quadratic optimization formulation and uses the barrier function method to derive algebraic state/input-dependent constraints for real-time optimization. Stability and optimal (or near-optimal) performance is shown for the proposed control.

The rest of paper is organized as follows. In section II, the class of saturated systems is introduced, and the control problem is defined. In section III, stability and robustness conditions under a general nonlinear control law are derived, the linear optimal tracker is introduced as the seed control, the barrier function method is applied to derive the algebraic state/input-dependent constraints, and the proposed nonlinear optimized control is solved in real-time from the corresponding point-wise constrained optimization problem. In section IV, the proposed control is applied to the microgrid control problem with high penetration of renewables. Then, conclusions are drawn in section V.

II. Problem Formulation

Consider the following class of dynamic systems with saturation on partial state (i.e., output), input and the rate of change of input:

$$\begin{cases} \dot{z} = A_z z + B_z \text{SAT}[u_z] + G_z r, \quad y_z = C_z z, \\ \dot{u}_z = \text{SAT}[u], \\ \eta_z = \text{SAT}[y_z], \end{cases} \tag{1}$$

R. Harvey and Z. Qu are with Department of Electrical and Computer Engineering, University of Central Florida, Orlando 32816, USA. T. Namerikawa is with Department of System Design Engineering, Keio University, Japan. Emails: *rharvey2@knights.ucf.edu*, *qu@ucf.edu*, and *namerikawa@sd.keio.ac.jp*. This work of the first two authors is supported in part by US National Science Foundation under grant ECCS-1308928, by US Department of Energy's awards DE-EE0007998, DE-EE0007327 and DE-EE0006340, and by US Department of Transportation's award DTRT13-G-UTC51.

This article has been accepted for publication in a future issue of this journal, but has not been fully edited. Content may change prior to final publication. Citation information: DOI 10.1109/LCSYS.2019.2929159, IEEE Control Systems Letters

where z is the original state vector, y_z is the unconstrained output, η_z is the constrained output, SAT[$\cdot$] denotes a vector of component-wise saturation functions, u_z is the control input vector subject to both magnitude and rate saturations, and $u \in \Re^m$ is the actual dynamic control to be synthesized. Matrices A_z, B_z, C_z and G_z are of appropriate dimensions. Exogenous input $r \in \Re^l$ is a function of time, and its historical value is recorded. Although the future value of $r(t)$ is typically unknown, its estimate $\hat{r}(t)$ could be generated using such technique as stochastic forecast [9], [10], [11].

By introducing the augmented state $x \in \Re^n$ and the overall constrained vector $\eta \in \Re^{p+m}$ as

$$x \triangleq [z^T \ u_z^T]^T, \quad \eta \triangleq [\eta_z^T \ \text{SAT}^T[u_z] \ \text{SAT}^T[u]]^T,$$

we can rewrite dynamics of system (1) as

$$\dot{x} = F(x,u) + Ax + Bu + Gr, \ y = C\eta, \ \eta = H(x,u), \quad (2)$$

subject to $\eta \in \Omega$, where

$$\Omega = \{\underline{c}_i \leq H_i(x,u) \leq \overline{c}_i, \quad i = 1, \cdots, (p+m)\} \quad (3)$$

$\underline{c}_i, \overline{c}_i$ are known lower and upper limits,

$$A = \begin{bmatrix} A_z & B_z \\ 0 & 0 \end{bmatrix}, \ B = \begin{bmatrix} 0 \\ I \end{bmatrix}, \ C^T = \begin{bmatrix} I \\ 0 \\ 0 \end{bmatrix}, \ G = \begin{bmatrix} G_z \\ 0 \end{bmatrix}, \quad (4)$$

y is the (unconstrained) output. Vector η consists of all variables subject to saturation, and function $F(x,u) : \Re^{n+m} \rightarrow \Re^n$ contains all the saturation-induced nonlinearities that vanish in set Ω. Specifically, elements of $F(x,u)$ are the nonlinear terms of saturated variables minus their unsaturated versions, i.e., $F(x,u) \equiv 0$ if $\eta \in \Omega$. It can be assumed in most applications that $\Omega \subset \Re^p$ is a compact set with $0 \in \Omega$.

The control problem solved in the paper consists of the following aspects:

- Analytical stability conditions are derived for nonlinear control system (2), and its robustness is established in the presence of forecasting error $(r - \hat{r})$.
- An optimal tracking control is developed for system (2) with respect to performance index

$$J = \frac{1}{2}\tilde{y}_f^T S_f \tilde{y}_f + \frac{1}{2}\int_{t_0}^{t_f} [\tilde{y}^T Q \tilde{y} + u^T R u] dt, \quad (5)$$

  where $\tilde{y} = y - y^d$, $y_f = C\eta(t_f)$, $S_f = S(t_f) \geq 0$, with y^d signifying the desired output. Square penalty matrices $Q \geq 0$ and $R > 0$ are symmetric and of appropriate dimensions. Although the nonlinear optimal control may not be solvable in general, a Lyapunov-based design is presented to force nonlinear system (2) to move in such a way that η gets into set Ω and remains there, hence the resulting control converges to the closed-form linear optimal solution.
- For any given set Ω, the constraints on η are handled by a barrier function design into which the aforementioned analytical optimal tracking control law is embedded.

III. Nonlinear and Optimal Controls

This section begins with a general nonlinear control design for system (2). The corresponding stability condition is derived using a combination of lemma 1 from [12] and the standard Lyapunov argument [13].

A. Nonlinear Control

While saturation functions are nonlinear, their Jacobians are piecewise constant. This observation leads us to use lemma 1 whose Lyapunov stability conditions are in terms of the Jacobian properties rather than the original nonlinear system. For the case that $\mathcal{V}$ is quadratic, lemma 1 can be used to conclude theorem 1.

Lemma 1 [12]: *Consider an error system in the form of $\dot{e} = \mathcal{F}(e,t)$, and assume that its Lyapunov function $\mathcal{V}(e,t)$ is positive definite and decrescent. If Jacobian matrix $\bigtriangledown_e \mathcal{F}$ has the property that*

$$\bigtriangledown_t \mathcal{V} + [\bigtriangledown_e \mathcal{V}]^T \ \bigtriangledown_w \mathcal{F}(w,t)|_{w=x-\delta e} \leq -\rho(\|e\|)$$

for some class-$\mathcal{K}$ function $\rho(\cdot)$, for all $x \in \Re^n$ and for all constants $\delta \in (0,1)$, then the system is uniformly asymptotically stable.

Theorem 1: *Consider system* (2) *under control*

$$u(x,t) = -R^{-1}B^T(k(x,t) - v(\hat{r},t)), \quad (6)$$

where v is a uniformly bounded function of $\hat{r}$ and time. Under control (6)*, denote $F(x,t) \triangleq F(x,u(x,t))$. If matrices $S(t)$ and*

$$\begin{aligned} \Gamma(w,t) \ \triangleq \ & \dot{S} + S \bigtriangledown_w [F(w,t) + Aw - BR^{-1}B^T k(w,t)] \\ & + \{\bigtriangledown_w [F(w,t) + Aw - BR^{-1}B^T k(w,t)]\}^T S \end{aligned}$$

are decrescent and positive definite for all $w \in \Re^n$, then system (2) *under control* (6) *has the following properties:*

- *If $\hat{r} = r$, the state is asymptotically convergent to equilibrium state x^e described by*

$$\begin{aligned} \dot{x}^e \ = \ & [F(x^e,u^e) + Ax^e - BR^{-1}B^T k(x^e,t)] \\ & + BR^{-1}B^T v(r,t) + Gr. \end{aligned} \quad (7)$$

- *If $\hat{r} \neq r$, the tracking error is input-to-state stable with respect to forecast error $(r - \hat{r})$*

where $u^e = u(x^e,t)$.

Proof: Under control (6), system (2) becomes

$$\dot{x} = [F(x,t) + Ax - BR^{-1}B^T k(x,t)] + BR^{-1}B^T v(\hat{r},t) + Gr.$$

If $\hat{r} = r$, the trajectory of equilibrium state x^e is governed by (7). Conversely, if $\hat{r} \neq r$, then for the state error $e = x - x^e$, we have the error system

$$\begin{aligned} \dot{e} \ = \ & [F(x,t) - F(x^e,t) + Ae \\ & + BR^{-1}B^T(-k(x,t) + k(x^e,t))] \\ & + BR^{-1}B^T(v(\hat{r},t) - v(r,t)). \end{aligned}$$

This article has been accepted for publication in a future issue of this journal, but has not been fully edited. Content may change prior to final publication. Citation information: DOI 10.1109/LCSYS.2019.2929159, IEEE Control Systems Letters

For positive definite matrix $S(t)$, we choose the Lyapunov function $\mathcal{V} = \frac{1}{2}e^T S(t)e$. It follows that, for some $\delta \in (0,1)$,

$$\begin{aligned}\dot{\mathcal{V}} &= \frac{1}{2}e^T S\dot{e} + \frac{1}{2}\dot{e}^T Se + \frac{1}{2}e^T \dot{S}e \\ &= e^T SBR^{-1}B^T[v(\hat{r},t) - v(r,t)] + \frac{1}{2}e^T\left[\Gamma|_{w=x-\delta e}\right]e \\ &\leq \lambda_{max}(SBR^{-1}B^T)\|e\|\|v(\hat{r},t) - v(r,t)\| \\ &\quad -\frac{1}{2}\lambda_{min}(\Gamma)\|e\|^2, \end{aligned} \tag{8}$$

where $\lambda_{max}(\cdot)$ and $\lambda_{min}(\cdot)$ denote the maximum and minimum eigenvalues, respectively, and from which asymptotic stability is seen from lemma 1 and input-to-state stability can also be concluded using [13]. ■

In general, there are many choices of $k(x,t)$ in feedback control (6). In the next subsection, an optimal control is presented as the seed control in the proposed design.

B. Optimal Control

In what follows, an optimal tracking control is derived for system (2) using standard techniques [14]. With respect to cost function (5), the Hamiltonian with costate $\lambda(t)$ is:

$$\mathcal{H} = \frac{1}{2}\tilde{y}^T Q\tilde{y} + \frac{1}{2}u^T Ru + \lambda^T(F(x,u) + Ax + Bu + G\hat{r}). \tag{9}$$

Then, the corresponding unconstrained optimization problem is to minimize the following cost function:

$$\overline{J} = \frac{1}{2}\tilde{y}_f^T S_f \tilde{y}_f + \int_{t_0}^{t_f}[\mathcal{H} - \lambda^T\dot{x}]dt. \tag{10}$$

It follows from calculus of variation [14], that the first-order variation of the cost function is given by

$$\begin{aligned}\delta\overline{J} &= (S_f\tilde{y}_f - \lambda_f^T)\delta x + \int_{t_0}^{t_f}\left[\left(\frac{\partial\mathcal{H}}{\partial x} + \dot{\lambda}\right)^T\delta x\right. \\ &\quad \left. + \left(\frac{\partial\mathcal{H}}{\partial u}\right)^T\delta u + \left(\frac{\partial\mathcal{H}}{\partial\lambda} - \dot{x}\right)^T\delta\lambda\right]dt, \end{aligned} \tag{11}$$

with $\lambda_f = S_f\frac{\partial\tilde{y}}{\partial x}|_{y=y_f}$. Upon $\delta\overline{J}$ in (11) being set to be zero, the following necessary conditions are obtained:

$$\begin{aligned}\dot{x} &= F(x,u) + Ax + Bu + G\hat{r} \\ \dot{\lambda} &= -\left(\frac{\partial y(x)}{\partial x}^T Q[y(x) - y^d] + \left[\frac{\partial F(x,u)}{\partial x} + A\right]^T\lambda\right) \\ u &= -R^{-1}\left[B + \frac{\partial F(x,u)}{\partial u}\right]^T\lambda \end{aligned}$$

with x_0 given. Comparing the above expression with control (6) of theorem 1, we know that, as long as $\text{SAT}[u] = u$, $\lambda = k(x,t) - v(\hat{r},t)$, and control (6) is also optimal if $k(x,t)$ and $v(\hat{r},t)$ are the solutions to the following equations:

$$\begin{aligned}\frac{\partial k(x,t)}{\partial t} &= -\frac{\partial k(x,t)}{\partial x}^T[F(x,u) + Ax - BR^{-1}B^Tk(x,t)] \\ &\quad -\frac{\partial y(x)}{\partial x}^T Qy(x) - \left[\frac{\partial F(x,u)}{\partial x} + A\right]^T k(x,t), \end{aligned} \tag{12}$$

$$\begin{aligned}\frac{dv(\hat{r},t)}{dt} &= \left[A - BR^{-1}B^T\frac{\partial k(x,t)}{\partial x} + \frac{\partial F(x,u)}{\partial x}\right]^T v(\hat{r},t) \\ &\quad -\frac{\partial k(x,t)}{\partial x}Gr + \frac{\partial y(x)}{\partial x}^T Qy^d; \end{aligned} \tag{13}$$

with terminal conditions $k(x_f,t_f) = S_f y_f$, $v(\hat{r},t_f) = S_f y^d$.

Although equations (12) and (13) can only be solved numerically in the general setting, they can be solved analytically whenever state η stays within set Ω as defined in (3). By parameterizing the solutions as $k(x,t) = S(t)x(t)$ and recalling $F(x,u) = 0$ for $\eta \in \Omega$, equations (12) and (13) reduce to the standard linear quadratic tracker:

$$\dot{S} = -SA - A^TS + SBR^{-1}B^TS - C^TQC \tag{14}$$

$$\dot{v} = [A - BR^{-1}B^TS]^Tv - SG\hat{r} + C^TQy^d \tag{15}$$

$$u^* = -R^{-1}B^T(Sx - v), \tag{16}$$

where (14) and (15) are solved backwards. The closed-form control (16) is only optimal for $\eta \in \Omega$. For $\eta \notin \Omega$, a stabilizing control can be designed according to theorem 1 and for system (2) whose nonlinearities consist of saturation functions. Specifically, linear optimal tracker (16) can always be embedded into control (6) with $v(\hat{r},t)$ given by (15) together with (14), and the nonlinear feedback control part $k(x,t)$ will be chosen to force η into set Ω and hence achieve both stability and optimality. This design, which utilizes barrier functions, is the topic of the next subsection.

C. Barrier Function Design

Based on input-output feedback linearization and a comparison argument, the so-called barrier function translates algebraic constraints on the output (including both the states variables and control u) into algebraic state-dependent inequalities in terms of the control. By satisfying such inequalities, the control can force output vector η into set Ω. By nature, such a control design ensures Lyapunov stability and, by making Ω an invariant set, control (6) becomes linear control (16) that achieves optimal performance within set Ω.

Definition 1: Consider system (2) with u satisfying its constraints and with $r = \hat{r}$ being a time-frozen value, expressed as $\dot{x} = f(x,\hat{r}) + Bu$, with barrier function $\xi_i(x)$. Then, an lth-order Lie derivative of $\xi_i(x)$ is recursively defined as

$$\begin{aligned}\mathcal{L}_f^{(1)}\xi_i(x) &= \frac{\partial\xi_i(x)}{\partial x}f(x,\hat{r}) \\ &\vdots \\ \mathcal{L}_f^{(l)}\xi_i(x) &= \frac{\partial}{\partial x}[\mathcal{L}_f^{(l-1)}\xi_i(x)]f(x,\hat{r}). \end{aligned}$$

The barrier function $\xi_i(x)$ is said to have relative degree μ_i if

$$\frac{\partial\xi_i(x)}{\partial x}B = 0, \quad \cdots \quad, \frac{\partial}{\partial x}[\mathcal{L}_f^{(l-2)}\xi_i(x)]B = 0,$$

This article has been accepted for publication in a future issue of this journal, but has not been fully edited. Content may change prior to final publication. Citation information: DOI 10.1109/LCSYS.2019.2929159, IEEE Control Systems Letters

and

$$\frac{\partial}{\partial x}[\mathcal{L}_f^{(l-1)}\xi_i(x)]B \neq 0.$$

Using the concept of relative degree, we can write high-order time derivatives of $\xi_i(x)$ as [13]: using differential operator s,

$$\xi_i^{(j)}(x) \triangleq s^j\xi_i(x) = \mathcal{L}_f^{(j)}\xi_i(x), \quad j = 1, ..., \mu_i - 1; \tag{17}$$

and

$$\xi_i^{(\mu_i)}(x) \triangleq s^{\mu_i}\xi_i(x) = \mathcal{L}_f^{(\mu_i)}\xi_i(x) + \frac{\partial}{\partial x}[\mathcal{L}_f^{(l-1)}\xi_i(x)]Bu. \tag{18}$$

The following lemma based on the comparison theorem provides the mechanism of employing a set of barrier functions, denoted by $\xi_i(x) \leq 0$ for $i = 1, \cdots, 2p$, into a nonlinear control design. In the remainder of the section, we denote $\xi_i(t) \triangleq \xi_i(x(t))$ to simplify the notation.

Lemma 2: Consider the following differential inequality:

$$\prod_{j=1}^{\mu_i}(s + \gamma_{ij})\xi_i(t) \leq 0, \tag{19}$$

where $\gamma_{ij} > 0$ are constants. Then, solution $\xi_i(t)$ has the property $\xi_i(t) \leq 0$ for all the time provided that $\xi_i(0) \leq 0$ and the following inequalities hold whenever $\mu_i > 1$:

$$\prod_{j=1}^{k}(s + \gamma_{ij})\xi_i(t)\Big|_{t=0} \leq 0, \quad \forall k \in \{1, \cdots, \mu_i - 1\}, \tag{20}$$

If $\xi_i(0) \not\leq 0$, then $\xi_i(t) \leq 0$ becomes true exponentially under inequality (19).

Proof: Differential inequality (19) can be expressed as

$$\alpha_l = (s + \gamma_{il})\alpha_{l-1}, \ j = 1, \cdots, \mu_i, \tag{21}$$

where $\alpha_0(t) = \xi_i(t)$, and $\alpha_{\mu_i}(t) \leq 0$. The solution to (21) is

$$\alpha_{l-1}(t) = \alpha_{l-1}(0)e^{-\gamma_{il}t} + e^{-\gamma_{il}t}\int_0^t e^{\gamma_{il}\tau}\alpha_l(\tau)d\tau, \tag{22}$$

from which we see that $\alpha_l(t) \leq 0$ and $\alpha_{l-1}(0) \leq 0$ imply $\alpha_{l-1}(t) \leq 0$. Hence, by induction, we know that the first statement of the lemma is true.

Differential inequality (19) can also be expressed as the following equality:

$$\prod_{j=1}^{\mu_i}(s + \gamma_{ij})\xi_i(t) = \alpha_{\mu_i}(t),$$

where $\alpha_{\mu_i}(t) \leq 0$. The above differential equation is asymptotically stable and hence, no matter what are the initial conditions, solution $\xi(t)$ will eventually become negative as solution (22) shows that $\alpha_{\mu_i-1}(t)$ will exponentially approach to negative values and by induction so will $\alpha_0(t)$. This proves the second statement of the lemma. ■

The specific steps of designing an optimized nonlinear control using barrier functions are as follows:

Step 1: It follows from (3) that there are a total of $2p$ state-dependent constraints. Choose their corresponding barrier functions as:

$$\xi_{2i-1} = H_i(x) - \overline{c}_i, \quad \xi_{2i} = \underline{c}_i - H_i(x), \quad i = 1, \cdots, p;$$

and determine the relative degree μ_i for each of ξ_i.

Step 2: Choose positive constants γ_{ij} for $j = 1, \cdots, \mu_i$ and calculate the corresponding characteristic polynomial:

$$\Delta_i(s) \triangleq \prod_{j=1}^{\mu_i}(s + \gamma_{ij}) = s^{\mu_i} + \sum_{j=0}^{\mu_i-1}\beta_j s^j. \tag{23}$$

It follows from the above expression and equation (18) that

$$\alpha_{\mu_i} = \frac{\partial}{\partial x}[\mathcal{L}_f^{(\mu_i-1)}\xi_i(x)]Bu + \mathcal{L}_f^{(\mu_i)}\xi_i(x) + \sum_{j=0}^{\mu_i-1}\beta_j\mathcal{L}_f^{(j)}\xi_i(x).$$

We know from lemma 2 that barrier $\xi_i(x) \leq 0$ can be ensured either all the time or asymptotically by choosing u such that the control as

$$\frac{\partial}{\partial x}[\mathcal{L}_f^{(\mu_i-1)}\xi_i(x)]Bu \leq -\mathcal{L}_f^{(\mu_i)}\xi_i(x) - \sum_{j=0}^{\mu_i-1}\beta_j\mathcal{L}_f^{(j)}\xi_i(x). \tag{24}$$

Step 3: The proposed nonlinear control (6) is the solution to the following real-time optimization: with u^* given by (16),

$$\begin{aligned} &u = \underset{u}{\operatorname{argmin}} \ \|u - u^*\|^2 \\ &\text{subject to } \begin{cases} (24) \text{ for } i = 1, \cdots, 2p; \\ u_i \in [\underline{c}_{p+i}, \ \overline{c}_{p+i}] \ \text{ for } \ i = 1, \ldots, m. \end{cases} \end{aligned} \tag{25}$$

The proposed control (25) is generally not nonlinearly optimal (in the spirit of (12) and (13)). The control is both near optimal and analytical in the presence of the constraints on the output, the input and its rate of change, and it does become optimal once η enters set Ω. Stability under the proposed design is given by the following theorem.

Theorem 2: *Consider system* (1) *in which matrix A_z is Lyapunov stable and the pair $\{A_z, \ B_z\}$ is controllable. Suppose that, with respect to the augmented nonlinear system* (2)*, η_i are input-output feedback linearizable with relative degree μ_i and with Lyapunov stable internal dynamics [13]. Then, nonlinear control* (25) *is Lyapunov stabilizing. If the reference signal y^d is feasible for system* (2) *with $\eta \in \Omega$, control* (25) *is also asymptotically stabilizing.*

Proof: It follows from (4) that A is Lyapunov stable if and only if A_z is Lyapunov stable and that $\{A, B\}$ is controllable if and only if $\{A_z, B_z\}$ is controllable. Hence, linear optimal control u^* in (16) is stabilizing and optimal for system (2) whenever $\eta \in \Omega$. On the other hand, control (25) forces η to move toward Ω exponentially and hence is stabilizing (in the sense of ensuring boundedness under any exogenous signal $r(t)$ and its (good) forecast $\hat{r}(t)$). As shown in lemma 2, Ω is also an invariant set in the sense that, once η moves into Ω, it will stay there. Therefore, if the reference signal y^d is achievable under the saturated controls, control (25) will make η to move into Ω, and hence the control is asymptotically stabilizing. ■

It is worth noting that, since the controls (and their rates of change) are saturated, trajectory y^d is feasible if both its magnitude and rate of change are limited. For the same reason, the exogenous signal $r(t)$ can be fully compensated if its magnitude and rate of change are also limited. As y^d and $r(t)$ become larger or faster, performance of the

This article has been accepted for publication in a future issue of this journal, but has not been fully edited. Content may change prior to final publication. Citation information: DOI 10.1109/LCSYS.2019.2929159, IEEE Control Systems Letters

overall system becomes degraded (gradually and graciously). Asymptotic stability could be lost but not Lyapunov stability (i.e., boundedness around the equilibrium).

IV. Application to Microgrid Control

The proposed design framework is motivated by the contemporary microgrid power control problem. In its simplest setting, a microgrid consists of the following components [15]: (i) An aggregated net load r, which is the total non-adjustable load minus distributed generation from solar and wind. (ii) A battery storage device of power output P_b and stored energy E:

$$\dot{P}_b = -\text{SAT}[u_b], \quad \dot{E} = P_b, .$$

(iii) A demand response (DR) program that adjusts controllable load P_{dr}:

$$M_l \dot{P}_{dr} = -P_{dr} + u_{dr}.$$

And, (iv) a traditional generator described by the swing equation together with turbine and governor control:

$$\begin{aligned} M_g \dot{x}_g &= -x_g + u_g, \\ M_s \dot{P}_m &= \text{SAT}(x_g - P_m), \\ M\dot{\omega} &= -D\omega + P_m - P_b - r - P_{dr}, \end{aligned}$$

where x_g is turbine output, P_m is mechanical power, and ω is frequency. M_l, M_g, M_s, M and D are system parameters.

The main control objective is to maintain the system frequency by balancing the load and generation and to optimize the system operation under a full set of input and output constraints. The output constraints are the maximum frequency range, the ramping rate of P_m, the limit on P_{dr}, and the operational range of battery storage, as listed below:

$$\begin{aligned} \omega &\in [\omega_0 - 0.05,\ \omega_0 + 0.05], \\ |(x_g - P_m)| &\in [0,\ c_{r,\max}] \\ |P_{dr}| &\le \overline{P}_{dr} \\ E &\in [0,\ \overline{E}], \end{aligned} \tag{26}$$

where ω_0 is the nominal frequency. Among the three control inputs, battery charging/discharging rate u_b is bounded as $u_b \in [\underline{u}_b,\ \overline{u}_b]$ while governor control input u_g and DR input u_{dr} are unconstrained.

If r were known in advance and its change were not too quick or overly large, a standard tracking control design would work. However, renewable resources are inherently uncertain, and while advanced data analytics methodologies can be used to forecast their values, intermittency and high variability are inevitable. This is illustrated by figure 1 drawn using the photovoltaics (PV) data from [16] and at the level of 100% PV penetration. In the figure, the net power data is in per unit, with 8MW as the base. The net load profile (in thick black) can be well-predicted [9], [10], [11] (as $\hat{r}$) but not the rapid changes (in red) due to solar generation variations. Those large swings make the microgrid control problem very challenging due to all the constraints explained above. In particular, the traditional generator can provide substantial power but its rate of change is slow. Demand response (i.e., load reduction) is relatively faster, but controllable loads are limited and load reduction incurs cost. Battery storage is fast, but its capacity must be limited due to cost, and its charging/discharging rates have to be constrained. As such, the proposed control is used as a coordinated optimal control strategy designed specifically to maintain frequency stability under the large transient disturbances and under existing input and output constraints.

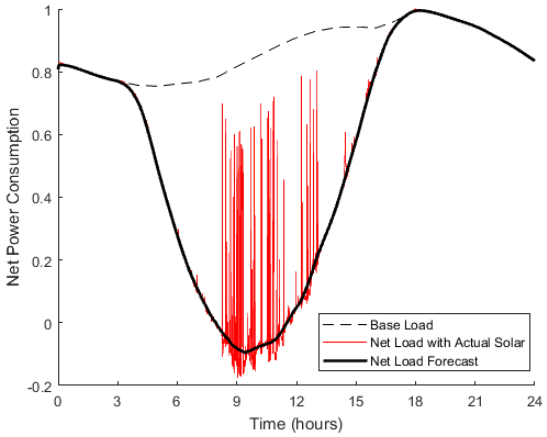

Fig. 1: Net load: the profile and large transient swings

To illustrate the performance of the proposed control, a simulation study is performed with the following parameters: $\omega_0 = 60$ Hz, $c_{r,\max} = 0.22$, $\overline{P}_{dr} = 0.1$, $\overline{E} = 0.07$, $\underline{u}_b = -0.1$, and $\overline{u}_b = 0.1$. For linear optimal tracker (16), $y^d = [(x_g^* - P_m^*)\ \omega_0\ 0\ \overline{E}/2]^T$, where x_g^* and P_m^* are free, penalty matrices are chosen to be $R = \text{diag}\{1, 20, 10\}$ (with respect to control vector $[u_g\ u_{dr}\ u_b]^T$) and $Q = \text{diag}\{0, 500, 250, 200\}$ (with respect to state vector $[(x_g - P_m)\ \omega\ P_{dr}\ E]^T$) so that their perspective control/state values are consistent with the control objective. In particular, minimizing frequency deviation is the top priority, thus its penalty is the highest among those for all the state variables.

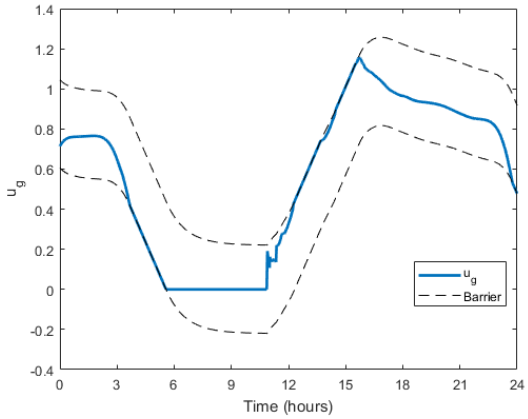

Fig. 2: Trajectory of u_g and its limiting values

Figure 2 shows the trajectory of u_g as well as the limiting values of u_g, which are calculated from barrier functions formed according to constraint (26). It is apparent that, during

This article has been accepted for publication in a future issue of this journal, but has not been fully edited. Content may change prior to final publication. Citation information: DOI 10.1109/LCSYS.2019.2929159, IEEE Control Systems Letters

the periods of the net load profile changes rapidly, control u_g makes the ramping rate reach but not exceed its boundary. Nonetheless, u_g is incapable of compensating for the large swings in PV generation.

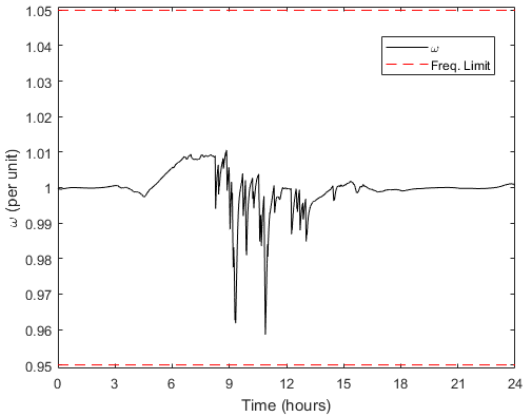

Fig. 3: Trajectory of system frequency

As revealed in figures 3 and 4, rapid ramping/dropping of net load (during 6-9am) and large intermittent changes of PV generation (during 8:30am to 2pm) are successfully compensated for by the combination of battery storage and DR. When the net load becomes negative even after conventional generation is turned off, battery and DR must be used to absorb the excess power. Battery power reaches its limit between 6-9am, and DR becomes the only asset to be controlled, which is due to the relative weights used in the optimal control design. Between 8:30am-2pm, both battery and DR compensate for the large swings of PV generation without letting the frequency drift out of its operational range. In short, the three control inputs are coordinated optimally such that all the constraints are satisfied at all times, including frequency stability.

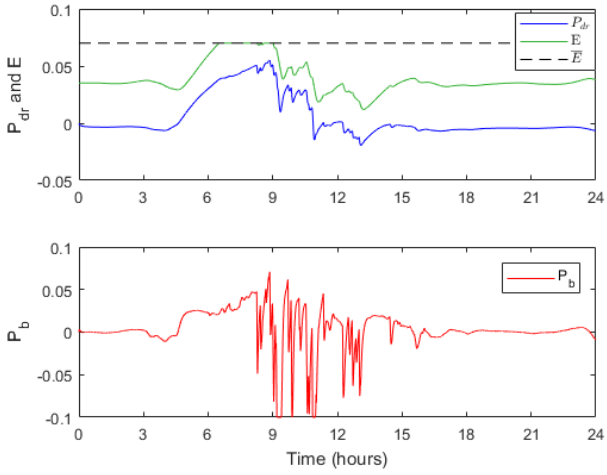

Fig. 4: Trajectory of battery and DR responses

V. Conclusion

In this paper, a nonlinear control design is presented for systems that are subject to saturation constraints on the system output, the system input, and the input rate of change. The proposed control employs barrier functions to explicitly take into account and enforce all the constraints, and it embeds a linear optimal control as the seed controller into a real-time optimization with dynamic and state-dependent constraints. Analytical stability conditions in terms of the piecewise-constant Jacobian matrix are obtained for systems with saturations, and the proposed control is shown to be stabilizing and ensure near-optimal or optimal performance with respect to a standard performance index. The proposed control is applied to the microgrid control problem in which traditional generation, battery storage, and demand response are subject to their perspective ramping rate and capacity constraints. The proposed control effectively coordinates the assets under their constraints and achieves frequency stability in the presence of rapid changes in renewable generation.

References

[1] K. van Berkel, R. Titulaer, T. Hofman, B. Vroemen, and M. Steinbuch, "From optimal to real-time control of a mechanical hybrid powertrain," *IEEE Transactions on Control Systems Technology*, vol. 23, no. 2, pp. 670–678, 2014.

[2] J. Biggs and W. Holderbaum, "Optimal kinematic control of an autonomous underwater vehicle," *IEEE transactions on automatic control*, vol. 54, no. 7, pp. 1623–1626, 2009.

[3] A. T. Tran, S. Suzuki, and N. Sakamoto, "Nonlinear optimal control design considering a class of system constraints with validation on a magnetic levitation system," *IEEE Control Systems Letters*, vol. 1, no. 2, pp. 418–423, 2017.

[4] H. Dagdougui, A. Ouammi, and R. Sacile, "Optimal control of a network of power microgrids using the pontryagin's minimum principle," *IEEE Transactions on Control Systems Technology*, vol. 22, no. 5, pp. 1942–1948, 2014.

[5] C. Feller and C. Ebenbauer, "A barrier function based continuous-time algorithm for linear model predictive control," in *2013 European Control Conference (ECC)*. IEEE, 2013, pp. 19–26.

[6] J. Hauser and A. Saccon, "A barrier function method for the optimization of trajectory functionals with constraints," in *Proceedings of the 45th IEEE Conference on Decision and Control*. IEEE, 2006, pp. 864–869.

[7] P. Glotfelter, J. Cortés, and M. Egerstedt, "Nonsmooth barrier functions with applications to multi-robot systems," *IEEE control systems letters*, vol. 1, no. 2, pp. 310–315, 2017.

[8] X. Xu, "Constrained control of input–output linearizable systems using control sharing barrier functions," *Automatica*, vol. 87, pp. 195–201, 2018.

[9] H. V. Haghi and Z. Qu, "Stochastic distributed optimization of reactive power operations using conditional ensembles of V2G capacity," in *Proceedings of American Control Conference*. IEEE, 2015, pp. 3292–3297.

[10] K. G. Boroojeni, M. H. Amini, S. Bahrami, S. Iyengar, A. I. Sarwat, and O. Karabasoglu, "A novel multi-time-scale modeling for electric power demand forecasting: From short-term to medium-term horizon," *Electric Power Systems Research*, vol. 142, pp. 58–73, 2017.

[11] H. V. Haghi and Z. Qu, "A kernel-based predictive model of EV capacity for distributed voltage control and demand response," *IEEE Transactions on Smart Grid*, vol. 9, no. 4, pp. 3180–3190, July 2018.

[12] Z. Qu, "Robust state observer and control design using command-to-state mapping," *Automatica*, vol. 41, no. 8, pp. 1323–1333, 2005.

[13] H. K. Khalil, *Nonlinear Systems*, 3rd ed. Prentice Hall New Jersey, 2003.

[14] F. L. Lewis, D. Vrabie, and V. L. Syrmos, *Optimal Control*. John Wiley & Sons, 2012.

[15] R. Harvey, Z. Qu, and T. Namerikawa, "Coordinated optimal control of constrained ders," in *IEEE Conference on Control Technology and Applications (CCTA)*. IEEE, 2018, pp. 224–229.

[16] "Hourly load data archives." [Online]. Available: http://www.ercot.com/gridinfo/load/load_hist/